Laser Fluence Dependence of the Electrical Properties of MoO$_2$ Formed by High Repetition Femtosecond Laser Pulses

Santiago Camacho-Lopez,* Israel O. Perez-Lopez, Miroslava Cano-Lara, Alejandro Esparza-Garcia, M. Carmen Maya-Sanchez, J. Apolinar Reynoso-Hernandez, and Marco Camacho-Lopez*

Molybdenum oxides have gained attention in the last few years due to their vast variety of polymorphs. These materials relate to technological applications in several devices to exploit their chromic and electrical features, among others. Molybdenum oxide (MoO$_2$ and Mo$_4$O$_{11}$) tracks are obtained in molybdenum thin films, deposited on glass substrates, by a previously reported (by our research group) optical technique based on femtosecond pulses from a Ti:sapphire laser oscillator. The present work reports on both the electrical resistance and resistivity of MoO$_2$ tracks as a function of the per pulse laser fluence (F_p) used for the oxide synthesis. It is found that the electrical resistance, as well as the resistivity, of the MoO$_2$ tracks drops as the delivered laser fluence is increased. The resistivity was determined to drop from $1.7 \times 10^{-3}\,\Omega\,cm$ to $5 \times 10^{-4}\,\Omega\,cm$. This result agrees well with resistivity measurements reported in the literature for MoO$_2$ nanosheets and films, respectively. This is explained by the fact that at low laser fluence the MoO$_2$ forms a very thin surface layer, while for high laser fluences the MoO$_2$ will get thick.

1. Introduction

Molybdenum oxides (MoO$_x$, $2 \leq x \leq 3$) present physical and chemical properties, which basically depend on both the oxygen content and the crystalline structure. A wide range of molybdenum oxides exists: m-MoO$_2$ (rutile type structure), Mo$_4$O$_{11}$ (orthorhombic, monoclinic), Mo$_{17}$O$_{47}$, Mo$_5$O$_{14}$, Mo$_8$O$_{23}$, Mo$_9$O$_{26}$, and MoO$_3$ (orthorhombic, monoclinic, high pressure, hexagonal phases).[1–12] In particular, these oxides have found applications in areas as: catalysis, gas sensors, lithium micro-batteries, supercapacitors, smart windows among other devices.[13–17] Up to now a-MoO$_3$ has been the most studied material of the whole selection of molybdenum oxides. However, it is still necessary to characterize the electrical properties of most of the MoO$_x$ ($2 \leq x < 3$) to enlarge and find new applications of these molybdenum oxides.

The well-known a-MoO$_3$ is a semiconductor material with a layered orthorhombic structure, while m-MoO$_2$ is a semimetal material with a rutile-type structure.[11,6] a-MoO$_3$ has found applications as a sensor material. In fact, a-MoO$_3$ thin films have been proven to be very sensitive to various gases such as NO, NO$_2$, CO, H$_2$, and NH$_3$ in the temperature

Dr. S. Camacho-Lopez, Dr. I. O. Perez[+] Dr. M. Cano-Lara[++]
Departamento de Óptica, Centro de Investigación Científica y de Educación Superior de Ensenada
Carretera Ensenada-Tijuana 3918, Zona Playitas, Ensenada, Baja California 22860, México
E-mail: camachol@cicese.mx

A. Esparza-Garcia
Fotofísica y Películas Delgadas, Departamento de Tecnociencias, Centro de Ciencias Aplicadas y Desarrollo Tecnológico, UNAM
Circuito Exterior s/n, Cd. Universitaria, Ciudad de Mexico 04510, Mexico

[iD] The ORCID identification number(s) for the author(s) of this article can be found under https://doi.org/10.1002/pssa.201800226.

[+]Current address: Department of Physics and Mathematics, Universidad Autonoma de Ciudad Juarez, Av. del Charro 450 Nte., Col. Partido Romero, Ciudad Juarez, Juarez Chihuahua, 32310, Mexico.
[++]Current address: Instituto Tecnologico Superior de Irapuato, Carretera Irapuato-Silao Km. 12.5, Irapuato, Guanajuato, 36821, Mexico.

Dr. M. C. Maya-Sanchez, Dr. J. A. Reynoso-Hernandez
Departamento de Electronica y Telecomunicaciones, Centro de Investigación Científica y de Educación Superior de Ensenada
Carretera Ensenada-Tijuana 3918, Zona Playitas, Ensenada, Baja California 22860, México

Dr. M. Camacho-Lopez
Laboratorio de Investigación y Desarrollo de Materiales Avanzados, Facultad de Química, Universidad Autónoma del Estado de México Campus Rosedal, Km 14.5 Carretera Toluca-Atlacomulco, San Cayetano de Morelos, Toluca C.P. 50295, México
E-mail: macamacholo@uaemex.mx

range from 300 to 600 °C.[14] Another family of materials based on α-MoO$_3$ with interesting properties in terms of applications are 2D MoO$_3$ nanoflakes, 2D MoO$_{3-x}$ nanosheets and H$_x$MoO$_3$ nanodisks. 2D MoO$_3$ nanoflakes films have been tried for protein biosensing, in particular using bovine serum albumin. While, 2D MoO$_{3-x}$ nanosheets have been shown to possess properties for electrocatalytic hydrogen evolution reaction. Recently, H$_x$MoO$_3$ nanodisks with plasmonic properties have been studied aiming to implement a glucose biosensor.[18–20] MoO$_2$ is an interesting material for various applications due to its electrical properties. This oxide is of great interest to be used as anode in lithium ion batteries.[21] It can be obtained as single crystal, powder, thin films, and various nanostructures as: ultrathin nanosheets, etc.[6–8,22] Nowadays, several methods have been employed to obtain MoO$_2$. For instance, molybdenum dioxide powder has been obtained by chemical reduction of MoO$_3$ or through the hydrothermal method. While MoO$_2$ thin films are usually fabricated by deposition methods like pulsed laser deposition (PLD), pulsed injection-metal organic chemical vapor deposition, electrodeposition, sputtering and chemical reduction.[7,23–26] More demanding forms of MoO$_2$ like ultrathin nanosheets have been prepared by thermal evaporation in a controlled atmosphere.[27]

In a previous work we report, side-by-side Mo$_4$O$_{11}$–MoO$_2$–Mo$_4$O$_{11}$, rapid track formation by irradiation of molybdenum thin films with high repetition rate femtosecond (fs) laser pulses.[28–30] This is a unique technique to form on demand oxide patterns (linear segments, rings, etc.) on molybdenum, or any other metallic thin film, by means of the local oxidation induced by the femtosecond laser pulses. The oxygen content and the crystalline phase of synthesized MoO$_x$ are strongly dependent on the laser irradiation and ambient conditions.

In this work, we report on the study of the per pulse laser fluence dependence, of the electrical resistance and the resistivity, of MoO$_2$ tracks induced by high repetition rate femtosecond laser pulses. The type of synthesized molybdenum oxide was determined by microRaman spectroscopy, and the electrical characterization was carried out by the four lead method. We contrast our results to those reported in the literature for some known forms of MoO$_2$ finding good agreement.

2. Experimental Section

2.1. Growth of Mo Thin Films

Molybdenum thin films were grown on fused silica substrates at room temperature by the magnetron DC-sputtering technique. The cubic crystal structure of the as deposited Mo films was determined by a XRD Siemens D-5000 diffractometer, and the morphology was studied by scanning electron microscopy. The 500 nm film thickness was measured by profilometry.[28]

2.2. Femtosecond-Laser Processing of the Mo Thin Films

The Mo films were irradiated by using a Ti:sapphire laser oscillator with pulses of 60 fs time duration, up to 7 nJ per pulse, at 70 MHz repetition rate, and wavelength centered at 800 nm.

An attenuator to adjust the delivered per pulse energy was composed by a half-wave retarder plate and a cube polarizer. The on target delivered energy per pulse was varied from 2.3 nJ up to 3.5 nJ. The film irradiation was conducted, in ambient air, at normal incidence, and focusing down the slightly elliptical incident laser beam with an aspheric lens of 35 mm focal length. This yields an elliptically shaped beam waist with a FWHM (full width half maximum), minor and major axes, of 7.7 and 12 μm, respectively. The films were conveniently mounted on a computer controlled XYZ linear stage. **Figure 1** shows a schematic diagram of the experimental set up. We laser exposed the films in the form of a series of straight line tracks, about 2.5 mm long, by keeping a constant scan speed at 530 μm s^{-1} during the laser exposure. We used an on target per pulse energy as quoted above and, therefore, per pulse delivered fluence within the range from 3.2 mJ cm^{-2} up to 4.8 mJ cm^{-2}. Since the scan speed was constant, the on target integrated laser fluence was only function of the number of scans performed along the same path, four for the present study, and the delivered per pulse fluence. Groups of tracks about 2.5 mm long, and tens of microns wide, as the ones shown in **Figure 2**, were irradiated on the Mo films. These SEM (scanning electron microscopy) images, of the synthesized MoO$_x$, reveal that each track is constituted by a smooth surface with submicron grain size. For each group the delivered per pulse laser fluence was varied. **Figure 3** shows optical micrographs of the as laser-processed MoO$_x$ tracks (Figure 3a), and the post processed MoO$_x$ tracks (Figure 3b); the last were exposed to aqua regia (a mixture of nitric acid and hydrochloric acid) to dissolve the surrounding metallic film in order to prepare isolated MoO$_x$ tracks for the purpose of electrical measurements. In Figure 3c–f, we can see how the MoO$_x$ optical appearance changes when the per pulse laser fluence increases. At low laser fluence (Figure 3c) a MoO$_2$ yellow track is generated, then at higher laser fluences (Figure 3d and e) the track changes its stoichiometry and it acquires a purple coloration; to end up at the highest used laser fluence (Figure 3f) with a track composed by two very well defined distinct zones. These two zones correspond to MoO$_2$ (center of the track) and Mo$_4$O$_{11}$ (sides of the track), according to our current and previous Raman studies.[28] We must notice in Figure 3b that the characteristic yellow MoO$_2$ central zone in the tracks gets narrower as the per-pulse laser fluence increases (right to left in Figure 3b), i.e., the formation of Mo$_4$O$_{11}$ on the sides of the track limits the MoO$_2$ width. However, as a whole the tracks get wider with increasing per-pulse laser fluence (Figure 3c–f) as it is expected because of heat diffusion.

2.3. Electrical Characterization of MoO$_x$ Tracks

The electrical resistance of the MoO$_x$ tracks was determined by the well-established four-lead method. Two picoprobe 7–175 (GGB Industries Inc.) tungsten probes (point radius <5 μm) were plugged in to a 2602A Keithley constant-current power supply with built-in voltmeter. The two probes were both located along the laser-scanned track. The separation distance between the probes was 250 ± 10 μm as shown in **Figure 4**, and a varying current was applied between the two tips to register the corresponding voltage. As pointed out above, prior to these
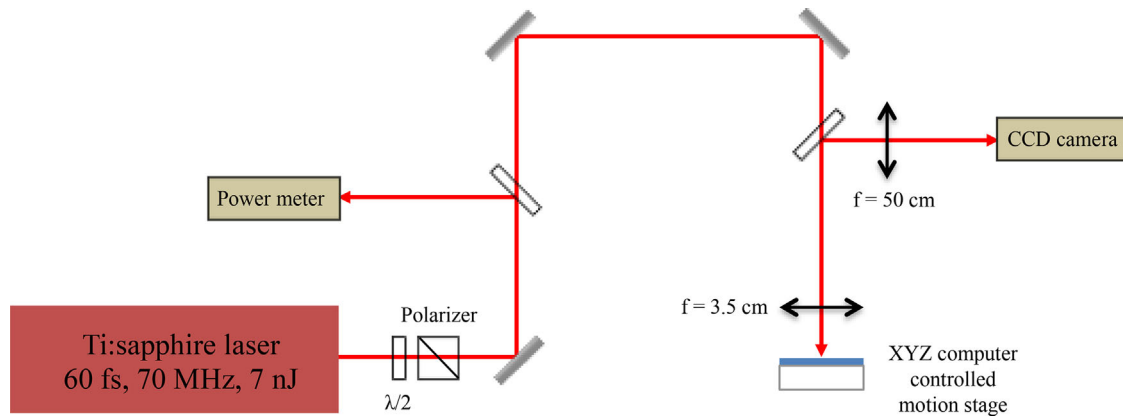
Figure 1. Experimental set up for MoO$_x$ synthesis through fs laser irradiation.

measurements, removing the surrounding metallic film (by aqua regia etching) conveniently isolated the MoO$_x$ tracks.

3. Results and Discussion

A visual inspection of the tracks in Figure 3a, b, and f and Figure 4b reveals the formation of two distinct zones, which are identified with MoO$_2$ in the central zone of the track, and Mo$_4$O$_{11}$ sideways.[28] Some of the tracks show crack defects caused during laser exposure (see Figure 4b). To avoid these defects when measuring the electrical features of the MoO$_x$ tracks, we selected small sections 250 μm long within the track. The Mo$_4$O$_{11}$ green-bluish side zone in the track forms as a result of heat diffusion and it occurs at high enough per pulse laser fluence.[28,30] **Figure 5** shows the Raman spectrum of the central zone, which proves the formation of MoO$_2$.

Voltage drop characterization measurements, carried out in the chosen locations on several tracks, showed that for a given current a narrower track produces a larger voltage drop than a wider track. Such fact suggests that the relevant quantity to be determined is not the resistance per length unit R, but the resistivity ρ of the MoO$_x$ tracks. The resistivity is given by the well-kown expression: $\rho = rA/l$, where r is the resistance, A is the
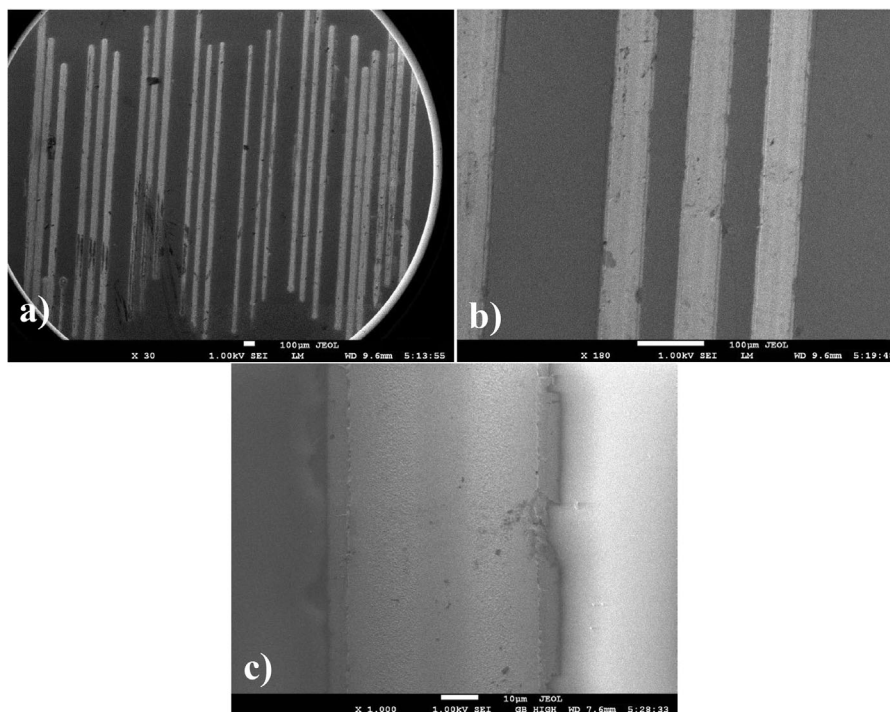

Figure 2. SEM images of the MoO$_x$ tracks obtained on the Mo films. a) Group of tracks obtained at different per pulse laser fluences; b) view of three tracks irradiated at the same per pulse laser fluence; c) zoom in for a single track, notice how the surface of the track is quite smooth with a very fine submicron grain size. The scale bars are 100 μm both in (a) and (b), and 10 μm in (c).
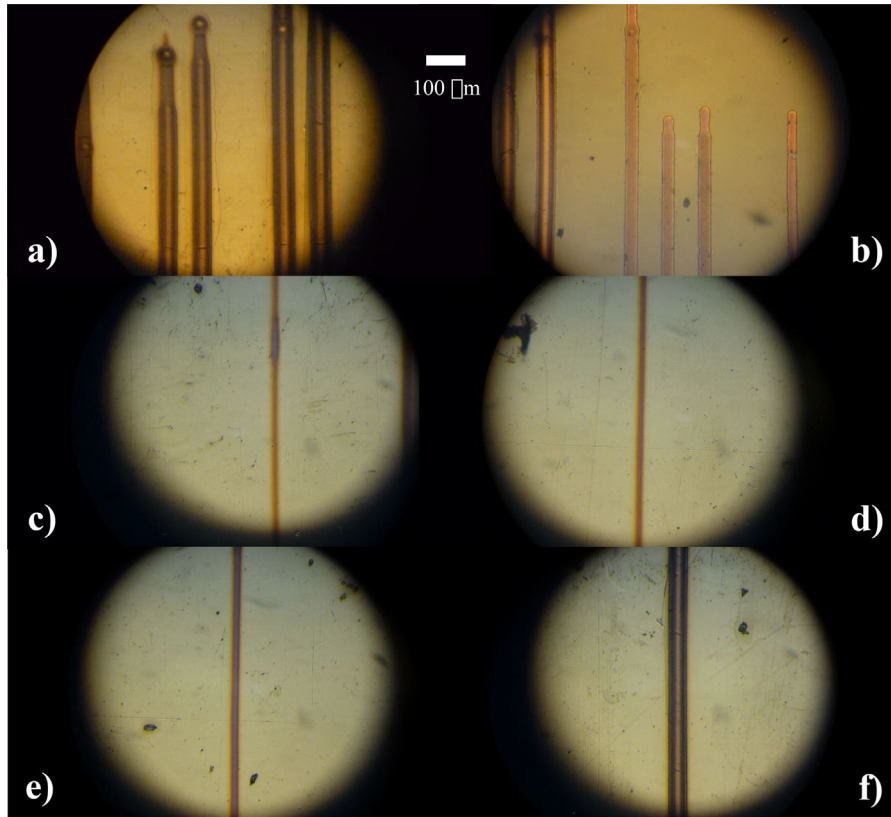
**ADVANCED
SCIENCE NEWS**

www.advancedsciencenews.com

pss**a**

physica status solidi

www.pss-a.com

Figure 3. Optical micrographs of the laser created track on the Mo film. a) The as synthesized MoO_x tracks; b) the MoO_x tracks after removing the surrounding metallic Mo through an acid bath; c–f) a sequence showing how the MoO_x evolves as the delivered per pulse laser fluence increases.

cross section of the conductor, and l is the conduction length. Notice that $R = r/l$ is the resistance per length unit.

Measurements of the resistance conducted in the center and the diffusion zones show minimum differences. **Figure 6** shows the current–voltage (I–V) average data for the center (MoO_2) and the diffusion (Mo_4O_{11}) zones for a group of tracks synthesized by using $4.8\,mJ\,cm^{-2}$ per pulse laser fluence. Both zones show an Ohmic behavior, this is not surprising since the two materials are known to possess either semimetal or metallic nature.[31] A linear fit of the data yields a resistance of 6.6 and $7.8\,\Omega$ for the center and the diffusion zones, respectively. For low per pulse

laser fluence the diffusion zone is negligible and the resistance corresponds only to the one due to MoO_2. The resistance per length unit for the central zone, i. e. the MoO_2 stripe, for all the processed tracks, as a function of increasing per pulse laser fluence monotonically drops. This same behavior for the resistance per length unit has also been reported for TiO_2 films, although the order of magnitude between the resistance of MoO_2 and TiO_2 significantly differs.[32]

In **Figure 7** we plot the resistivity for the studied MoO_2 tracks as function of the per pulse laser fluence. For this we computed the track cross section given by the thickness of the oxide layer
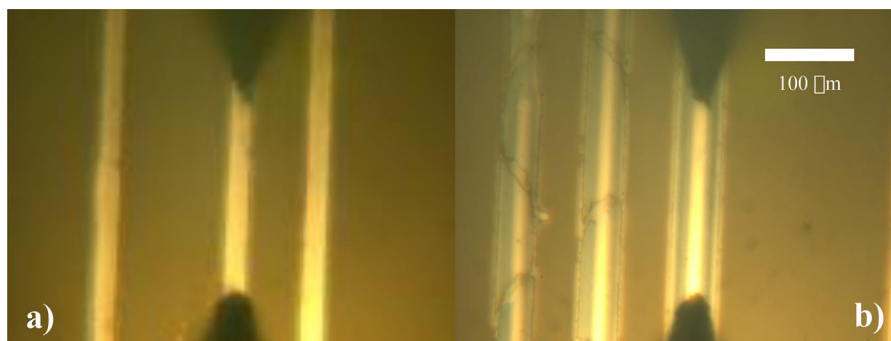

Figure 4. The two probes (dark triangular shapes) set on one of the MoO_2 tracks for I–V measurements. The distance between the tips of the probes is $250\,\mu m$. a) Low laser fluence track where MoO_2 prevails; b) high laser fluence track where MoO_2 and Mo_4O_{11} coexist.
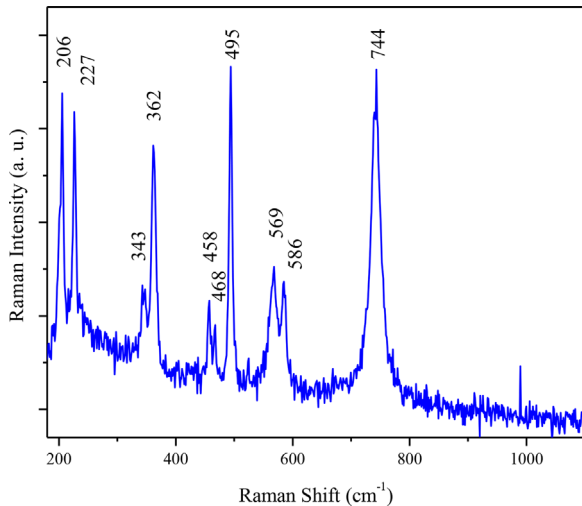
ADVANCED
SCIENCE NEWS

www.advancedsciencenews.com

physica
pss status solidi a

www.pss-a.com

Figure 5. Characteristic MoO_2 Raman spectrum obtained for the center of the track shown in Figure 4b.

Figure 7. Resistivity for MoO_2 as a function of the per pulse laser fluence.

times the width of the track, which varies with the delivered laser fluence. It can be seen how the resistivity also drops as it does the resistance per length unit. For computing the resistivity of the MoO_2 zone we take into account the following facts: the width of the MoO_2 decreases as the per-pulse laser fluence decreases from nearly 50 μm down to approximately 15 μm; the thickness of the formed MoO_2 layer grows from a few nanometers up to nearly several hundreds of nanometers, for the lowest to the highest per pulse laser fluences we used in the MoO_x synthesis. At low laser fluences the interaction is mainly confined to the optical penetration depth (20 nm in this case, since the absorption coefficient of Mo is $50 \times 10^4 \, cm^{-1}$), with limited oxygen diffusion depth into the Mo film; while at high laser fluences the heat diffusion favors oxygen diffusion along the full Mo film thickness. In the case of measuring the resistance of the very thin
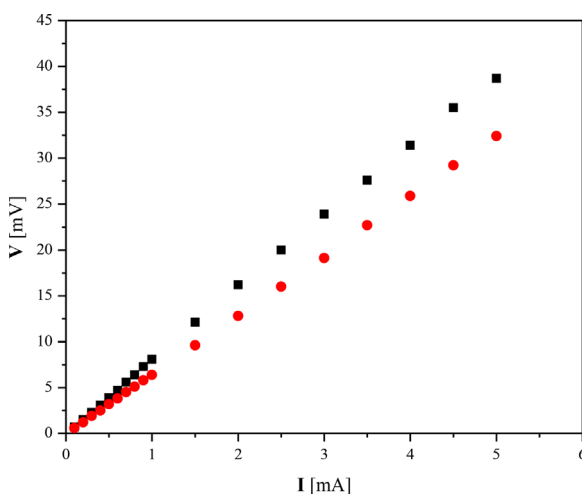
MoO_2 layer at the surface, the question arise of how the current keeps within that layer without going to the underlying layer. A possible explanation is that the underlying layer (MoO_{2-x}) possesses a density of point defects, which result from the limited oxygen diffusion at low laser fluences. It has been proven for femtosecond laser-induced ZnO that, low laser fluence exposure during synthesis produces a material with high density of point defects, this material with such point defects shows higher resistance than the one measured in the same material synthesized at higher fluences. [33] Therefore, if the MoO_2 top layer has low density point defects, or it is point defects free, and it is supported on top of a MoO_{2-x} layer with high density point defects, the MoO_2 must exhibit lower resistance than the underlying MoO_{2-x}. Our measurements produce a resistivity, which drops from $1.7 \times 10^{-3} \, \Omega \, cm$ down to $5 \times 10^{-4} \, \Omega \, cm$. The highest resistivity corresponds to the lowest per pulse laser fluence, while the lowest resistivity corresponds to the highest per pulse laser fluence. These measurements agree well with recently reported highly conductive MoO_2 nanosheets, with conductivity values in the range of $200–475 \, S \, cm^{-1}$ (resistivity in the order of $2–5 \times 10^{-3} \, \Omega \, cm$);[27] and resistivity values for MoO_2 thin films in the order of $7 \times 10^{-4} \, \Omega \, cm$.[23] We must point out that in our case at low per pulse laser fluence a very thin MoO_2 layer, only a few nanometers thick, must form; however, at higher per pulse laser fluences a thicker, several hundreds of nanometers, layer of MoO_2 should form. It is consistent then to obtain the resistivity we have experimentally determined for the MoO_2 tracks reported in the present study.

4. Conclusion

We have determined both the electrical resistance per length unit and the resistivity of femtosecond laser-induced MoO_2 tracks. We consistently found that the resistance per length unit decreases as the per pulse laser fluence used during the synthesis increases. The experimental results also showed that the resistance in the so named diffusion zone, where Mo_4O_{11} forms, is slightly higher than in the center MoO_2 zone. The laser

Figure 6. I–V measurements for the center (MoO_2) zone (red circles) and the diffusion (Mo_4O_{11}) zone (black squares) of the laser processed tracks. Linear fit of the experimental data produces a resistance of 6.6 Ω and 7.8 Ω for the center and the diffusion zones, respectively.
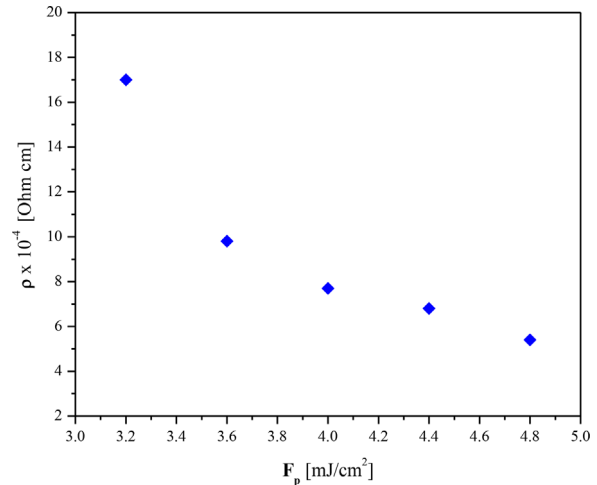
ADVANCED
SCIENCE NEWS
www.advancedsciencenews.com

physica
status
solidi
a
www.pss-a.com

fluence dependent resistivity for MoO_2, we report in the present work, is in very good agreement with the one reported in recent literature for MoO_2 nanosheets and MoO_2 films, which were synthesized by two different methods. Our findings are important in view of the multiple opto-electronic applications of molybdenum oxides, which include a variety of sensors, electrodes, and other devices.

Conflict of Interest

The authors declare no conflict of interest.

[1] E. R. Braithwaite, J. Haber, *Molybdenum: An Outline of Chemistry and Uses*. Elsevier, Amsterdam, The Netherlands **1994**.

[2] I. Alves de Castro, R. S. Datta, J. Z. Ou, A. Castellanos-Gomez, S. Sriram, T. Daeneke, K. Kalantar-zadeh, *Adv. Mater.* **2017**, *29*, 1701619.

[3] M. Dieterle, G. Weinberg, G. Mestl, *Phys. Chem. Chem. Phys.* **2002**, *4*, 812.

[4] M. Dieterle, G. Mestl, *Phys. Chem. Chem. Phys.* **2002**, *4*, 822.

[5] A. Blume, PhD Thesis, Technische Universität Berlin, Germany, **2004**.

[6] R. Srivastava, L. L. Chase, *Solid State Commun.* **1972**, *11*, 349.

[7] P. A. Spevack, N. S. McIntyre, *J. Phys. Chem.* **1992**, *96*, 9029.

[8] M. A. Camacho-Lopez, L. Escobar-Alarcon, M. Picquart, R. Arroyo, G. Cordoba, E. Haro-Poniatowski, *Opt. Mater.* **2011**, *33*, 480.

[9] M. Borovšak, P. Sutar, E. Goreshnik, D. Mihailović, *Appl. Surf. Sci.* **2015**, *354*, 256.

[10] P. F. García, E. M. McCarron III, *Thin Solid Films* **1987**, *155*, 53.

[11] E. M. McCarron III, *J. Chem. Soc. Chem. Commun.* **1986**, *0*, 336.

[12] C. I. Vargas-Consuelos, M. Camacho-Lopez, *Superficies y Vacío* **2014**, *27*, 123.

[13] A. Katrib, P. Leflaive, L. Hilaire, G. Maire, *Catal. Lett.* **1996**, *38*, 95.

[14] M. B. Rahmani, S. H. Keshmiri, J. Yu, A. Z. Sadek, L. Al-Mashat, A. Moafi, K. Latham, Y. X. Li, W. Wlodarski, K. Kalantar-zade, *Sens. Actuators B* **2010**, *145*, 13.

[15] G. Pistoia, *Lithium Batteries New Materials Developments and Perspectives*. Elsevier, The Netherlands **1994**.

[16] J. Rajeswari, P. S. Kishore, B. Viswanathan, T. K. Varadarajan, *Electrochem. Commun.* **2009**, *11*, 572.

[17] K. A. Gesheva, T. M. Ivanova, G. Bodurov, *Prog. Org. Coat.* **2012**, *74*, 635.

[18] S. Balendhran, S. Walia, M. Alsaif, E. P. Nguyen, J. Z. Ou, S. Zhuiykov, S. Sriram, M. Bhaskaran, K. Kalantar-zadeh, *ACS Nano.* **2013**, *7*, 9753.

[19] R. S. Datta, F. Haque, M. Mohiuddin, B. J. Carey, N. Syed, A. Zavabeti, B. Zhang, H. Khan, K. J. Berean, J. Z. Ou, N. Mahmood, T. Daeneke, K. Kalantar-zadeh, *J. Mater. Chem. A* **2017**, *5*, 24223.

[20] B. Yue Zhang, A. Zavabeti, A. F. Chrimes, F. Haque, L. A. O'Dell, H. Khan, N. Syed, R. Datta, Y. Wang, A. S. R. Chesman, T. Daeneke, K. Kalantar-zadeh, J. Zhen Ou, *Adv. Funct. Mater.* **2018**, *28*, 1706006.

[21] C. A. Ellefson, O. Marin-Flores, S. Ha, M. G. Norton, *J. Mater. Sci.* **2012**, *47*, 2057.

[22] O. de Melo, L. García-Pelayo, Y. González, O. Concepción, M. Manso-Silván, R. López-Nebreda, J. L. Pau, J. C. González, A. Climent-Fontae, V. Torres-Costa, *J. Mater. Chem. C* **2018**, *6*, 6799. https://doi.org/10.1039/C8TC01685B

[23] C. H. Ma, J. C. Lin, H. J. Liu, T. H. Do, Y. M. Zhu, T. D. Ha, Q. Zhan, J. Y. Juang, Q. He, E. Arenholz, P. W. Chiu, Y. H. Chu, *Appl. Phys. Lett.* **2016**, *108*, 253104.

[24] R. Narro-García, N. Méndez, L. M. Apátiga, J. P. Flores-De los Ríos, C. G. Nava-Dino, R. Quintero-Torres, *Int. J. Electrochem. Sci.* **2017**, *12*, 3907.

[25] N. Dukstiene, D. Sinkeviciute, A. Guobiene, *Cent. Eur. J. Chem.* **2012**, *10*, 1106.

[26] Y. Liu, H. Zhang, P. Ouyang, W. Chen, Y. Wang, Z. Li, *J. Mater. Chem. A* **2014**, *2*, 4714.

[27] E. Pu, D. Liu, P. Ren, W. Zhou, D. Tang, B. Xiang, Y. Wang, J. Miao, *AIP Adv.* **2017**, *7*, 025015.

[28] M. Cano-Lara, S. Camacho-López, A. Esparza-García, M. A. Camacho-López, *Opt. Mater.* **2011**, *33*, 1648.

[29] N. Cuando-Espitia, J. Redenius, K. Mensink, M. Camacho-Lopez, S. Camacho-Lopez, G. Aguilar, *Opt. Mater. Express* **2018**, *8*, 581.

[30] M. Cano-Lara, PhD Thesis, CICESE, Mexico, **2012**.

[31] M. S. da Luz, A. de Campos, B. D. White, J. J. Neumeier, *Phys. Rev. B* **2009**, *79*, 233106.

[32] M. Tsukamoto, N. Abe, Y. Soga, M. Yoshida, H. Nakano, M. Fujita, J. Akedo, *Appl. Phys. A* **2008**, *93*, 193.

[33] Y. Esqueda-Barrón, M. Herrera, S. Camacho-López, *Appl. Surf. Sci.* **2018**, *439*, 681.